Computers, Materials & Continua

Tech Science Press

DOI: 10.32604/cmc.2023.037028
Article

A Universal Activation Function for Deep Learning

Seung-Yeon Hwang[1] **and Jeong-Joon Kim**[2,*]

[1]Department of Computer Engineering, Anyang University, Anyang-si, 14028, Korea
[2]Department of ICT Convergence Engineering, Anyang University, Anyang-si, 14028, Korea
*Corresponding Author: Jeong-Joon Kim. Email: jjkim@anyang.ac.kr
Received: 20 October 2022; Accepted: 15 January 2023

Abstract: Recently, deep learning has achieved remarkable results in fields that require human cognitive ability, learning ability, and reasoning ability. Activation functions are very important because they provide the ability of artificial neural networks to learn complex patterns through nonlinearity. Various activation functions are being studied to solve problems such as vanishing gradients and dying nodes that may occur in the deep learning process. However, it takes a lot of time and effort for researchers to use the existing activation function in their research. Therefore, in this paper, we propose a universal activation function (UA) so that researchers can easily create and apply various activation functions and improve the performance of neural networks. UA can generate new types of activation functions as well as functions like traditional activation functions by properly adjusting three hyperparameters. The famous Convolutional Neural Network (CNN) and benchmark dataset were used to evaluate the experimental performance of the UA proposed in this study. We compared the performance of the artificial neural network to which the traditional activation function is applied and the artificial neural network to which the UA is applied. In addition, we evaluated the performance of the new activation function generated by adjusting the hyperparameters of the UA. The experimental performance evaluation results showed that the classification performance of CNNs improved by up to 5% through the UA, although most of them showed similar performance to the traditional activation function.

Keywords: Deep learning; activation function; convolutional neural network; benchmark datasets; universal activation function

1 Introduction

Recently, deep learning has shown very good results in computer vision fields such as image classification [1–5], object recognition [6–11], object tracking [12,13], etc. with the help of large-capacity artificial intelligence learning data and high-end computing resources. In addition, research is being actively conducted in fields such as speech recognition [14–16] and natural language processing

[17–20]. The activation function is very important because it transfers the value extracted from the previously hidden layer to the input of the next layer for learning the artificial neural network. If an artificial neural network uses a linear function as an activation function, it has no meaning in deeply constructing the neural network, so it uses a nonlinear function as an activation function. That is, a model designed with a deep structure may function like a model without a hidden layer. Currently, various nonlinear functions such as Sigmoid [21], Hyperbolic tangent (Tanh) [22], Rectifier Linear Unit (ReLU) [23], Parametric ReLU (PReLU) [24], Randomized ReLU (RReLU) [25], Leaky ReLU (LReLU) [26], Swish [27], Exponential Linear Unit (ELU) [28] and others [29–32] are available as activation functions of artificial neural networks. By using these nonlinear functions as an activation function, it is possible to construct a deep neural network. However, with Sigmoid and tanh, it is not a serious problem in shallow artificial neural networks, but as the model deepens, the gradient becomes zero when updating numerous weights in the back propagation process of deep learning, resulting in a problem that learning no longer progresses. ReLU has been introduced to solve this vanishing gradient problem, but if most input values are in the negative range, the weight may not be updated while returning 0 to the output value of the activation function. To solve this Dying Node problem, several studies have been conducted, such as reducing the Learning Rate or modifying the ReLU. However, researchers need a lot of time and effort to apply and evaluate various existing activation functions in their own research. Therefore, in this paper, we propose a UA that can easily generate and implement a new type of activation function as well as an activation function similar to the traditional activation function. The UA uses three hyperparameters that determine the shape of the activation function according to the range of input values. Researchers can use various types of activation functions by appropriately modifying the three hyperparameters. The contribution goals to be achieved in this study through a UA are as follows.

- The UA is proposed to improve the usability of the activation function of the researcher and the performance of the existing neural network.
- The UA introduced the k, m, and L hyperparameters, allowing researchers to generate various activation functions.
- We evaluate UAs by implementing Visual Geometry Group (VGG) 16, VGG19, Residual Network (ResNet) 50, and CustomNet and show similar or better performance compared to traditional activation functions.
- Using CIFAR10, CIFAR100 [33] and Horses or Humans benchmark datasets with different classes and resolutions of images, we have secured the reliability of experimental performance evaluation and can be used in various areas.

The structure of this paper describes the related activation functions in Section 2 and the dataset to be used for experimental performance evaluation in Section 3. Section 4 describes the UA proposed in this study, and Section 5 describes the methods and results of experimental performance evaluation. Section 6 concludes this study.

2 Related Works

2.1 Sigmoid

Sigmoid was mainly used in early artificial neural networks and is also called a logistic function. Sigmoid began to be used to obtain nonlinear values from linear multi-perceptrons and can be expressed as Eq. (1). Sigmoid is limited to a value between 0 and 1, so a very large positive number has a value close to 1 and a very large negative number has a value close to 0. Sigmoid in shallow artificial neural networks is not a serious problem, but it can cause serious problems due to the vanishing gradient in which the gradient approaches zero as the model deepens. Due to these disadvantages, recently it has been only used for binary classification and not for hidden layers of models.

$$f(x) = \frac{1}{1 + e^{-x}} \tag{1}$$

2.2 ReLU

ReLU is proposed to solve the vanishing gradient problem of Sigmoid and Tanh. ReLU can be expressed as Eq. (2) and is an identity function for a positive input value and outputs 0 for a negative input value. This function has the advantage of speeding up the learning speed because it is easy to calculate the differential, but it may cause a dying node problem.

$$f(x) = \begin{cases} x, & (x > 0) \\ 0, & (x \leq 0) \end{cases} \tag{2}$$

2.3 Swish

Swish is an activation function devised by Google to replace ReLU and shows a simple form of multiplying the input by the sigmoid as shown in Eq. (3). Swish outperforms ReLU when training models in deep layers. By not limiting the range of output values in positive numbers, the vanishing gradient problem can be solved, and the dying node problem can be solved by allowing some small negative output values. And the output feature map responds small to small changes and large to large changes so that the optimizer can find the optimal minima.

$$f(x) = \frac{x}{1 + e^{-x}} \tag{3}$$

3 Datasets

The datasets used in the experiments in this study utilize one of the most used benchmark datasets, Canadian Institute for Advanced Research (CIFAR) 10, CIFAR100, and Horses or Humans. CIFAR10 consists of 10 classes, 32 × 32 images, 50,000 training images and 10,000 test images. The CIFAR100 consists of 100 classes, 32 × 32 images, 50,000 training images and 10,000 test images. Horses or Humans consists of two classes, 300 × 300 images, 1027 training images and 256 test images. Fig. 1 shows a dataset sample. Table 1 summarizes and shows the information of each data.

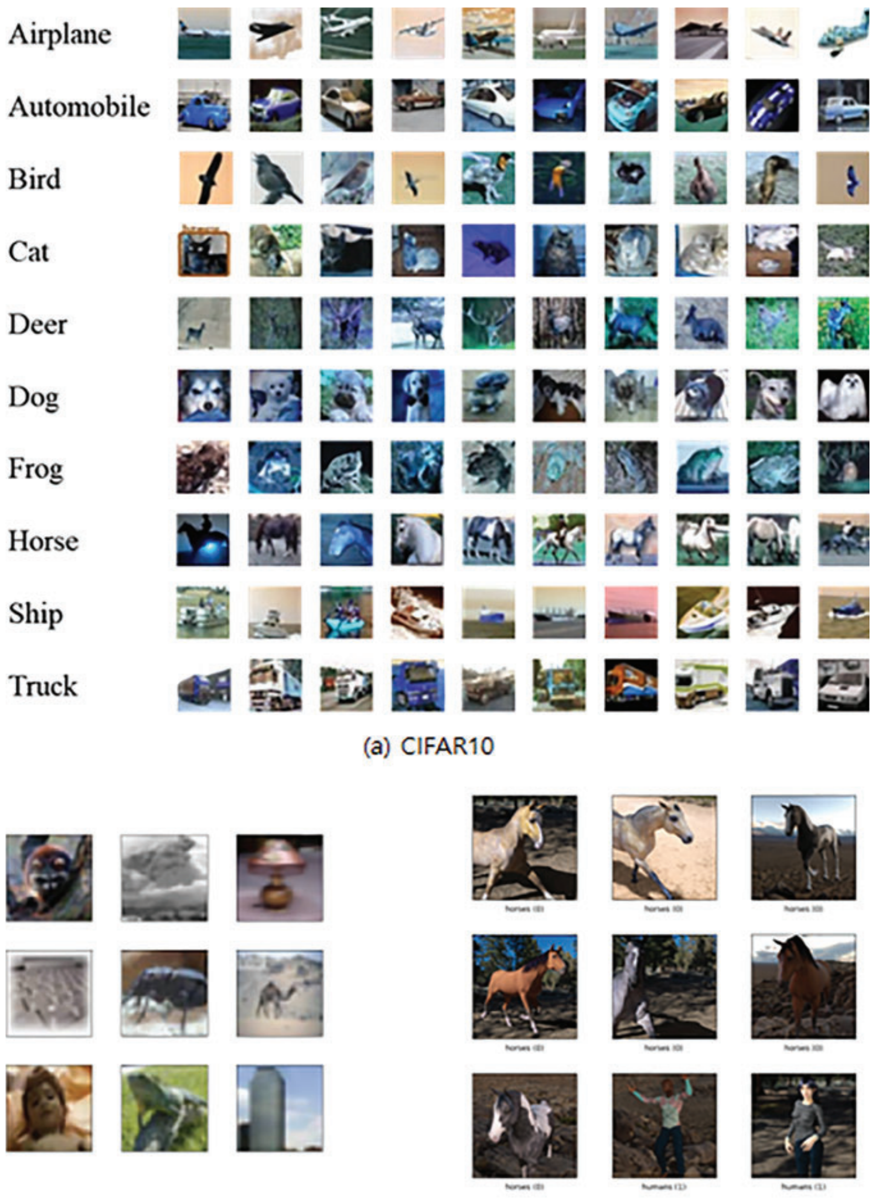

(b) CIFAR100 (c) Horses or Humans

Figure 1: Sample image of CIFAR10, CIFAR100, horses or humans dataset

4 Universal Activation Function

The formula for UA proposed in this paper is shown in Eq. (4).

$$\textit{Universal activation function}\,(x) = \begin{cases} x^k & x > L \\ x^k \dfrac{(L+x)^m}{(L+x)^m + (L-x)^m} & |x| \le L \\ 0 & x < -L \end{cases} \tag{4}$$

Table 1: Database information of CIFAR10, CIFAR100 and horses or humans

No.	Dataset	Training	Testing	Total	Classes
1	CIFAR-10	50,000	10,000	60,000	10
2	CIFAR-100	50,000	10,000	60,000	100
3	Horses or humans	1,027	256	1,283	2

The x of a UA means the input value, and the k, m, and L hyperparameters determine the form of the activation function. The value of k determines the shape of the graph of the interval in which the input value is greater than L. The value of m gently adjusts the shape of the graph so that the value of the slope does not change rapidly. The value of L is the criterion for dividing the activation function into three intervals. Researchers can set three parameters appropriately to generate a desired type of activation function. And a visualizer was developed to visualize these activation functions. The visualizer allows visualization by selecting the desired activation function among Swish, Sigmoid, ReLU, and ELU, and when UA is selected, a graph of the activation function is output according to the applied hyperparameters. Figs. 2–4 show the ReLU, Sigmoid, and Swish activation functions generated using a UA through the visualizer.

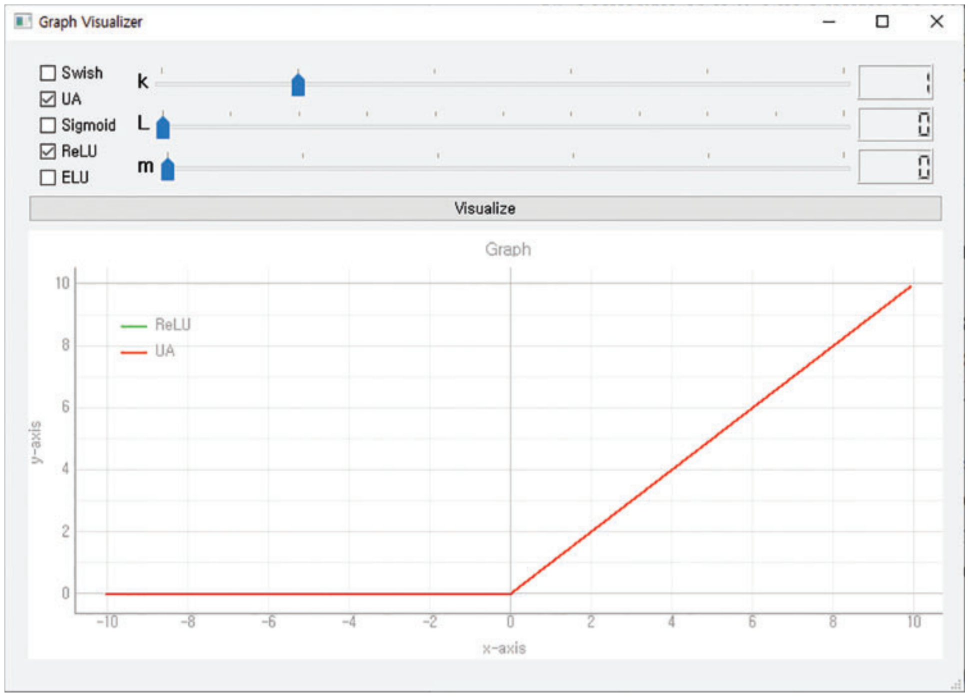

☐ Swish
☑ UA
☐ Sigmoid
☑ ReLU
☐ ELU

k 1
L 0
m 0

Figure 2: ReLU generated using UA

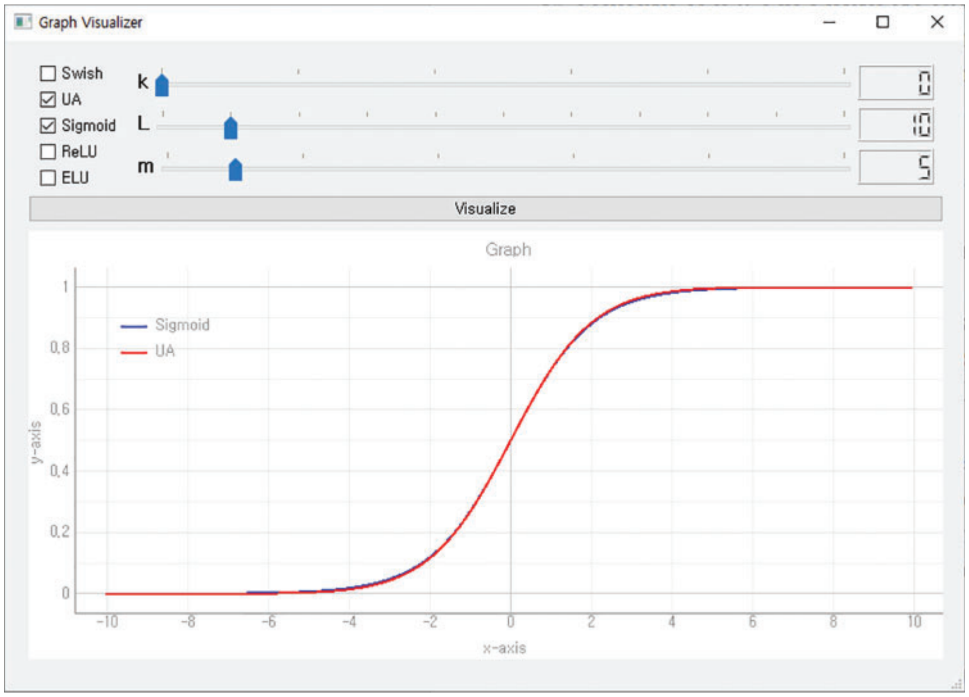

Graph Visualizer

- [ ] Swish
- [✓] UA
- [✓] Sigmoid
- [ ] ReLU
- [ ] ELU

k 0

L 10

m 5

Figure 3: Sigmoid generated using UA

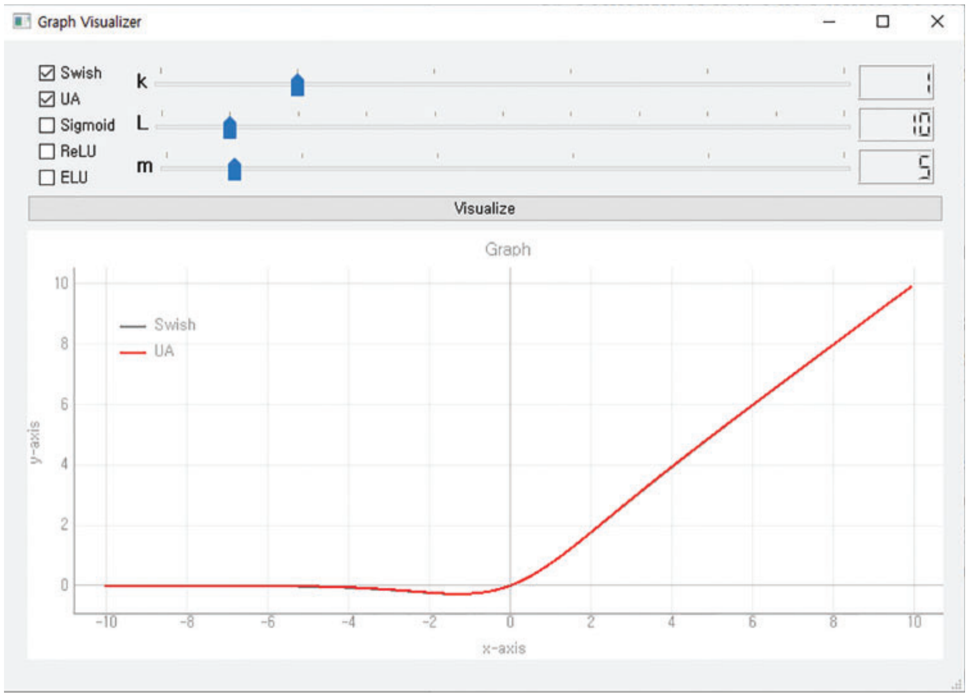

Graph Visualizer

- [✓] Swish
- [✓] UA
- [ ] Sigmoid
- [ ] ReLU
- [ ] ELU

k 1

L 10

m 5

Figure 4: Swish generated using UA

To check the similarity between the traditional activation function and the UA, the output vector of the activation function for random input vector was calculated and the results were prepared in Table 2.

Table 2: Comparison of input/output between traditional activation functions and UAs

Input tensor	Traditional activation function	Traditional Activation Function Output tensor (TAO)	UA	UA Output tensor (UAO)	Difference (TAO–UAO)
−0.05060163	ReLU	0.	UA-ReLU	0.	0.
0.46190243		0.46190244		0.46190244	0.
−0.43726205		0.		0.	0.
−0.62066391		0.		0.	0.
0.7539121		0.7539121		0.7539121	0.
	Sigmoid	0.4873523	UA-Sigmoid	0.4873521	0.0000002
		0.61346537		0.6135434	−0.00007803
		0.39239353		0.39232722	0.00006631
		0.34963048		0.34944883	0.00018165
		0.6800305		0.6803422	−0.0003117
	Swish	−0.02466082	UA-Swish	−0.02466081	−0.00000001
		0.28336114		0.2833972	−0.00003606
		−0.17157881		−0.17154981	−0.000029
		−0.217003		−0.21689026	−0.00011274
		0.5126832		0.51291823	0.00023503

According to Table 2, for any input vector, ReLU and UA-ReLU have the same output vector. In the case of sigmoid and swish, there are some errors, but it is proved that there are no performance issues through experimental performance evaluation. The UA proposed in this paper can generate various types of activation functions as well as functions like traditional activation functions by adjusting three parameters. Therefore, various researchers will be able to easily use the activation function by changing the parameters to create an activation function suitable for the data and research purpose.

5 Experimental Performance Evaluation

5.1 Environment and Method

The activation function visualizer developed in this study was developed in Windows 10 with Python programming language. Experimental performance evaluation was performed in Docker container of Ubuntu 20.04 OS and implemented using Python programming language and Keras library. The hardware of the PC consists of an NVIDIA GeForce Ray Tracing (RTX) 3080 GPU, an Advanced Micro Devices (AMD) Ryzen 7 5700X CPU and 64 GB of RAM.

For the experimental performance evaluation of the UA, a custom neural network consisting of three Conv layers, three Pooling layers, and one fully connected layer was utilized to minimize the value lost as the neural network deepens, as well as CNN won the ImageNet Large Scale Visual Recognition Challenge (ILSVRC). The architecture of CustomNet is shown in Fig. 5. All three Conv layers used

3×3 filters, and MaxPool layers used 2×2 filters. The Conv1 layer used 32 kernels, the Conv2 layer used 64 kernels, and the Conv3 layer used 128 kernels. The output vector dimension of the FC1 layer was set to 256.

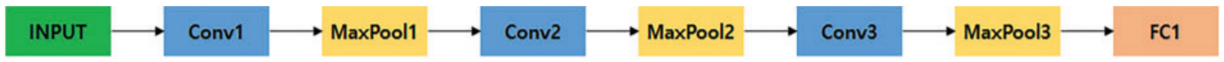

Figure 5: CustomNet model architecture

The CIFAR10, CIFAR100, Horses or Humans datasets were used to evaluate the experimental performance of this study, and the hyperparameters applied to each neural network are shown in Table 3.

Table 3: Hyperparameters based on neural networks and data

Neural network	Dataset	Learning rate	Optimizer	Epoch	Batch size
VGG16	CIFAR-10	0.00001	Adam	50	64
VGG19	CIFAR-100	0.00001	Adam	50	64
	Horses or humans	0.00001	Adam	50	32
ResNet50	CIFAR-10	0.0001	Adam	50	64
CustomNet	CIFAR-100	0.0001	Adam	50	64
	Horses or humans	0.0001	Adam	50	32

To confirm the performance according to the activation function, the weight decay scheduler was not used for the learning rate, and a CNN model that was not pre-trained was used. And Adam Optimizer [34] was used for fast weight convergence. Additionally, we used the CIFAR10 dataset to perform an experimental performance evaluation based on changes in hyperparameters that determine a UA.

5.2 Results and Analysis

5.2.1 Experimental Performance Evaluation Results for CIFAR-10

Table 4 shows the results of learning the CIFAR10 using traditional activation functions (ReLU, Swish) and UAs (UA-ReLU, UA-Swish). Fig. 6 is a visualization for intuitive understanding of the results.

The results show that the validation accuracy of the traditional activation function and the UA is mostly derived similarly for the entire model. For ResNet50, UA-ReLU has improved accuracy by about 5.3% compared to ReLU. The reason why ResNet50 is less accurate than other neural networks is that the neural network is composed of layers deeper than the resolution of a given dataset, so it is judged that it has not been learned normally because many features of the image have been lost in the hidden layer.

Table 4: Classification accuracy for CIFAR10 of CNN according to activation function

Model	Traditional activation function	Validation accuracy on traditional activation function	UA	Validation accuracy on UA
CustomNet	ReLU	74.58	UA-ReLU	75.52
	Swish	72.13	UA-Swish	71.41
VGG16	ReLU	84.56	UA-ReLU	84.32
	Swish	84.68	UA-Swish	84.71
VGG19	ReLU	84.13	UA-ReLU	83.54
	Swish	84.46	UA-Swish	84.15
ResNet50	ReLU	24.08	UA-ReLU	29.42
	Swish	61.65	UA-Swish	61.36

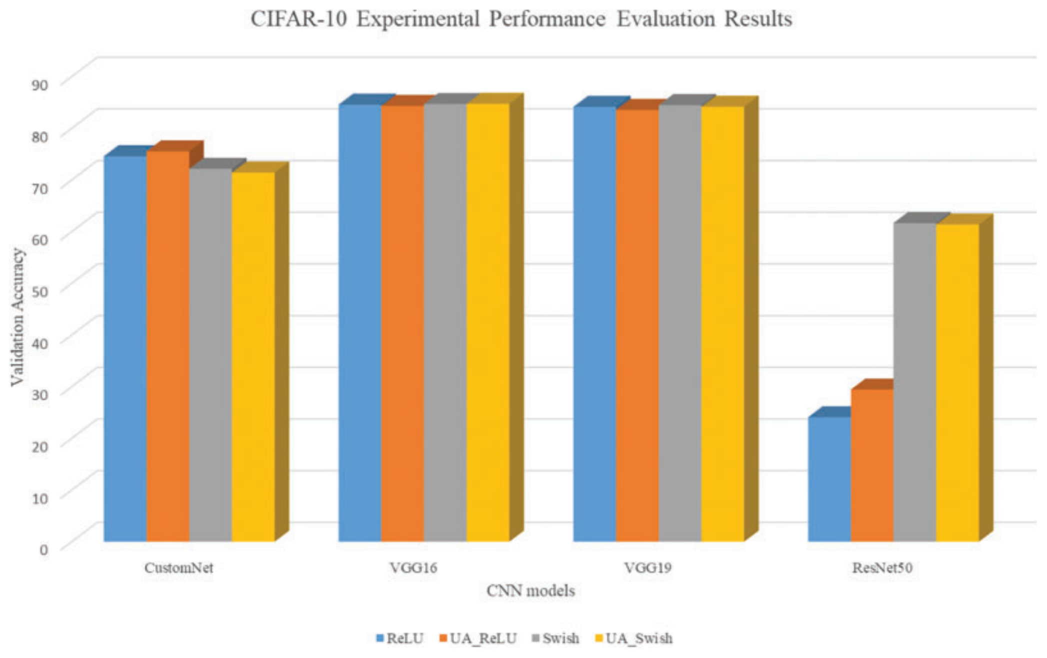

Figure 6: CIFAR10 results bar graph

5.2.2 *Experimental Performance Evaluation Results for CIFAR-100*

Table 5 shows the results of learning the CIFAR100 using traditional activation functions and UAs. Fig. 7 is a visualization for intuitive understanding of the results.

As a result of learning the CIFAR100 dataset, most of them show similar accuracy, and the accuracy is generally slightly higher when UA is applied. Like the CIFAR10 dataset, it is judged that the accuracy of ResNet50 is low because the resolution of the given dataset is low and many image features are lost in the hidden layer.

Table 5: Classification accuracy for CIFAR100 of CNN according to activation function

Model	Traditional activation function	Validation accuracy on traditional activation function	UA	Validation accuracy on UA
CustomNet	ReLU	42.82	UA-ReLU	43.26
	Swish	40.11	UA-Swish	41.10
VGG16	ReLU	58.78	UA-ReLU	58.33
	Swish	59.07	UA-Swish	59.57
VGG19	ReLU	56.38	UA-ReLU	56.73
	Swish	56.95	UA-Swish	56.80
ResNet50	ReLU	31.61	UA-ReLU	31.00
	Swish	35.42	UA-Swish	35.47

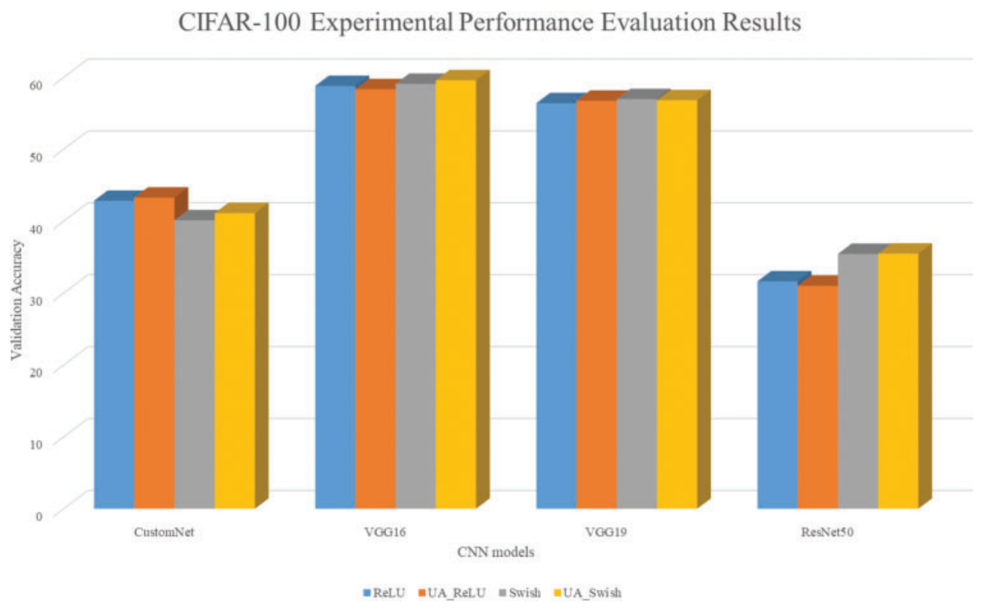

Figure 7: CIFAR100 results bar graph

5.2.3 *Experimental Performance Evaluation Results for Horses or Humans*

Table 6 shows the results of learning the Horses or Humans using traditional activation functions and UAs. Fig. 8 is a visualization for intuitive understanding of the results.

As a result of learning from the Horses or Humans dataset, CustomNet had higher accuracy when applying a UA. The VGG16 showed similar accuracy and the VGG19 showed similar accuracy for ReLU, but the accuracy was approximately 3.5% lower for UA-Swish. In the case of ResNet50, it is judged that it was not learned normally, such as the CIFAR10 and CIFAR100 dataset learning results.

Table 6: Classification accuracy for horses or humans of CNN according to activation function

Model	Traditional activation function	Validation accuracy on traditional activation function	UA	Validation accuracy on UA
CustomNet	ReLU	81.64	UA-ReLU	86.32
	Swish	85.93	UA-Swish	87.89
VGG16	ReLU	98.82	UA-ReLU	98.44
	Swish	98.43	UA-Swish	98.83
VGG19	ReLU	98.43	UA-ReLU	98.43
	Swish	96.09	UA-Swish	92.57
ResNet50	ReLU	75.00	UA-ReLU	50.00
	Swish	51.95	UA-Swish	50.00

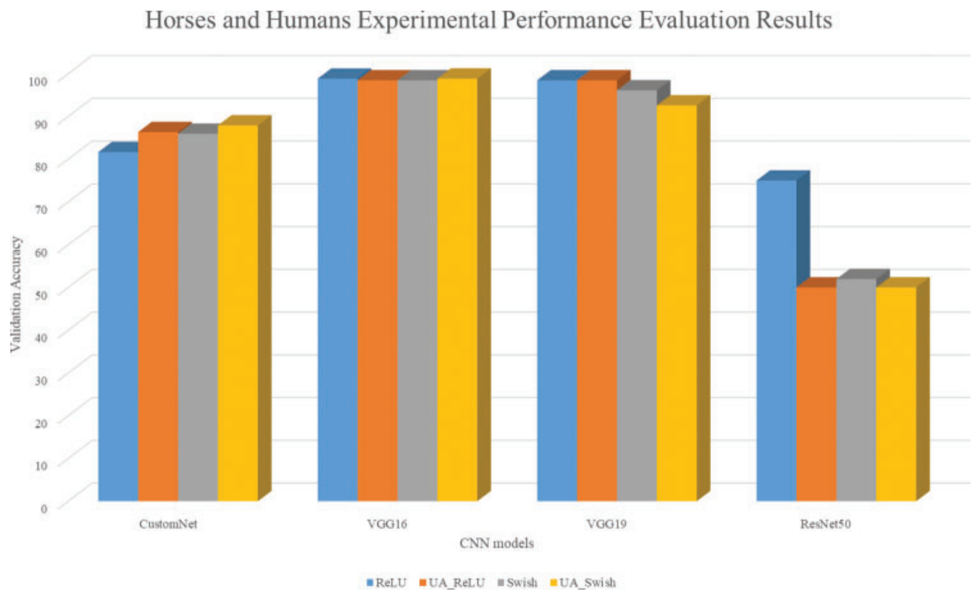

Figure 8: Horses or humans results bar graph

5.2.4 Experimental Performance Evaluation Results of UA According to Hyper-Parameter

Considering the diversity of the study, three hyperparameters of the UA were changed to generate activation functions similar to ELU not covered in the previous section, and the experimental performance evaluation was conducted using the CIFAR10 dataset. Table 7 shows the hyperparameters of the three UAs and the results of learning CIFAR10.

The hyperparameters of the first UA were set to $k = 1$, $m = 3$, and $L = 35$. Fig. 9 shows the first UA graph, and Fig. 10 visualizes the results.

The accuracy of the neural network to which the first general-purpose activation function was applied was found to be about 19.56% lower than the average accuracy of the model trained with four activation functions (ReLU, Swish, UA-ReLU, UA-Swish) for CustomNet. However, in the case of VGG16 and VGG19 neural networks, about 1.2% and 1.6% accuracy improvements were found. In the case of ResNet50, it seems that the image features are lost in the hidden layer, but there was a performance improvement of about 34.4% compared to the result of applying the four activation functions.

Table 7: Hyperparameters of UA and validation accuracy of each model

No.	k	m	L	CNN	Validation accuracy
1	1	3	35	CustomNet	53.85
2				VGG16	85.74
3				VGG19	85.66
4				ResNet50	78.48
5	1	5	44	CustomNet	53.55
6				VGG16	84.73
7				VGG19	84.96
8				ResNet50	77.56
9	1	1	17	CustomNet	76.6
10				VGG16	81.78
11				VGG19	79.21
12				ResNet50	77.74

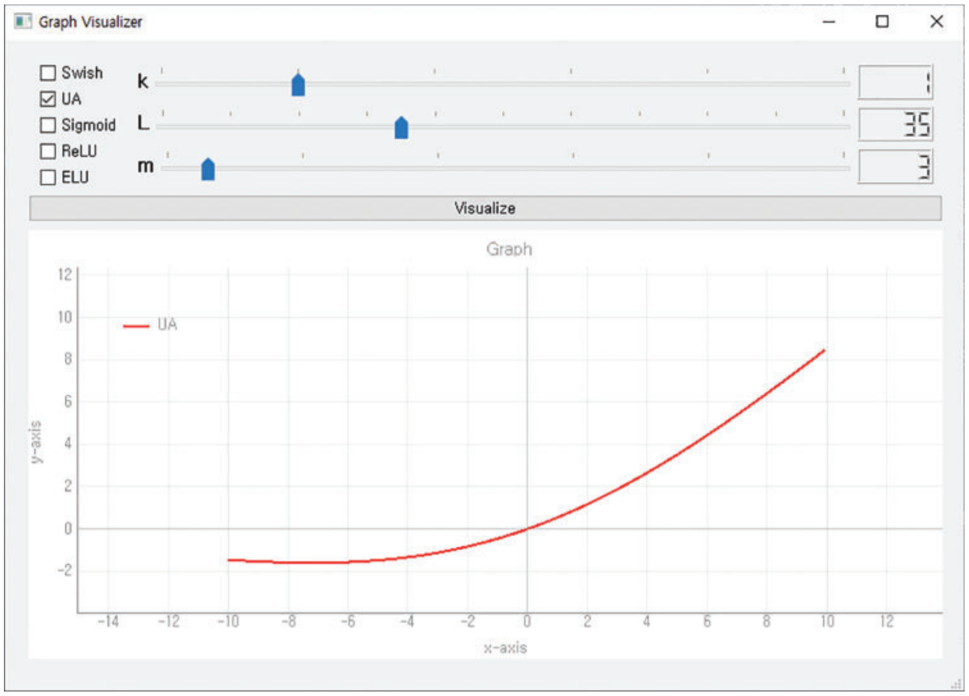
Graph Visualizer

☐ Swish
☑ UA
☐ Sigmoid
☐ ReLU
☐ ELU

k: 1
L: 35
m: 3

Figure 9: Graph of UA (k = 1, m = 3, L = 35)

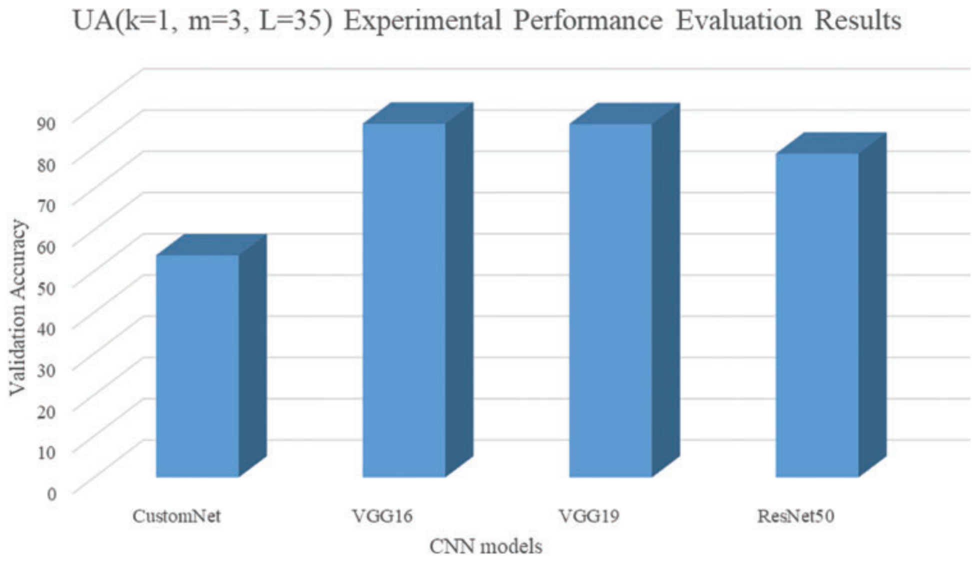

Figure 10: Results of UA (k = 1, m = 3, L = 35)

The hyperparameters of the second UA were set to k = 1, m = 5, and L = 44. Fig. 11 shows the second UA graph, and Fig. 12 visualizes the results.

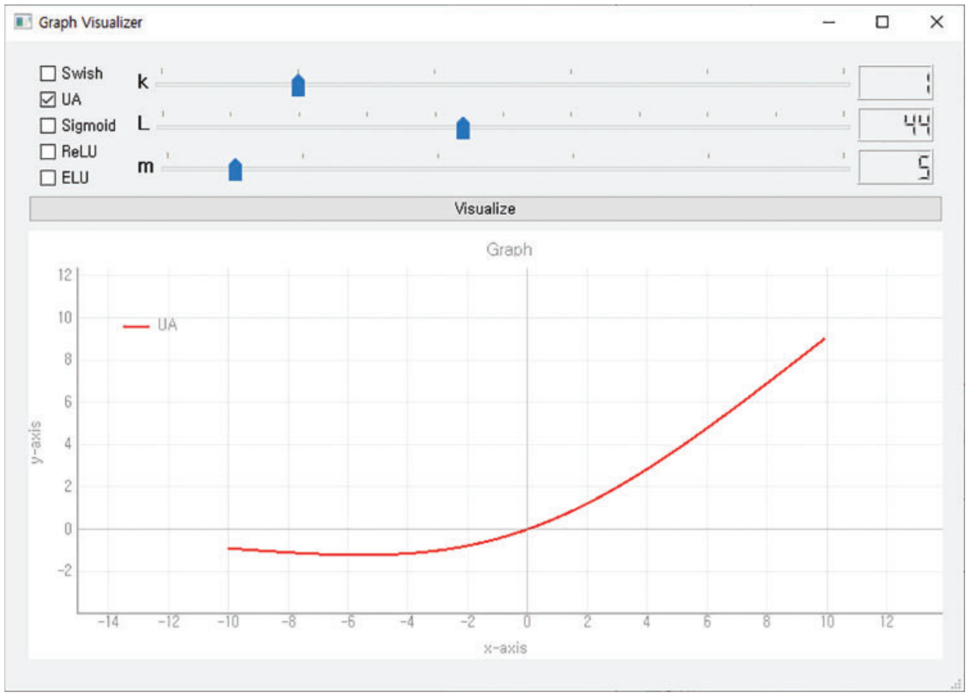

Figure 11: Graph of UA (k = 1, m = 5, L = 44)

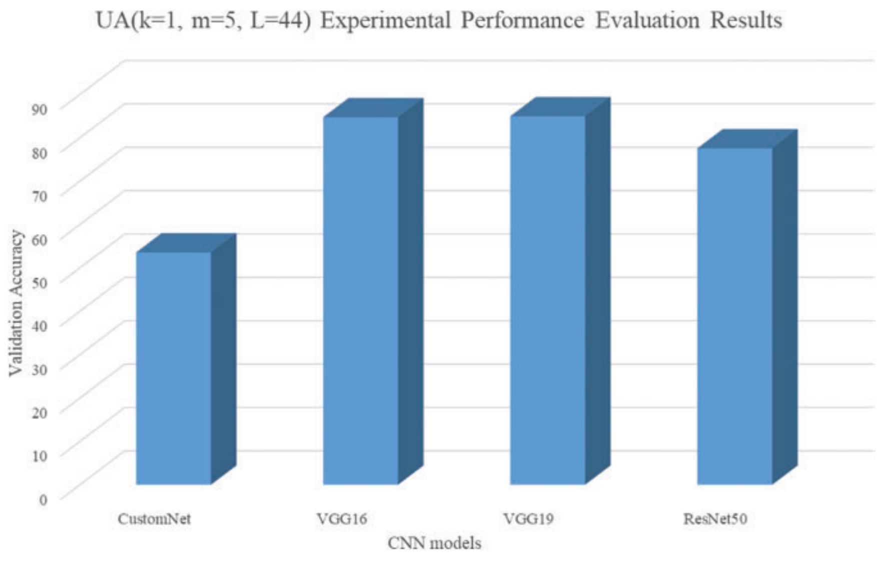

Figure 12: Results of UA (k = 1, m = 5, L = 44)

The accuracy of applying the second UA was like that of the first UA applied to CustomNet. In the case of VGG16 and VGG19, there was a slight improvement in performance compared to the four activation functions, but the case of applying the first UA showed better accuracy. ResNet50 also had the loss of image features of the hidden layer, but there was a performance improvement of about 33.4%.

The hyperparameters of the third UA were set to k = 1, m = 1, and L = 17. Fig. 13 shows the third UA graph, and Fig. 14 visualizes the results.

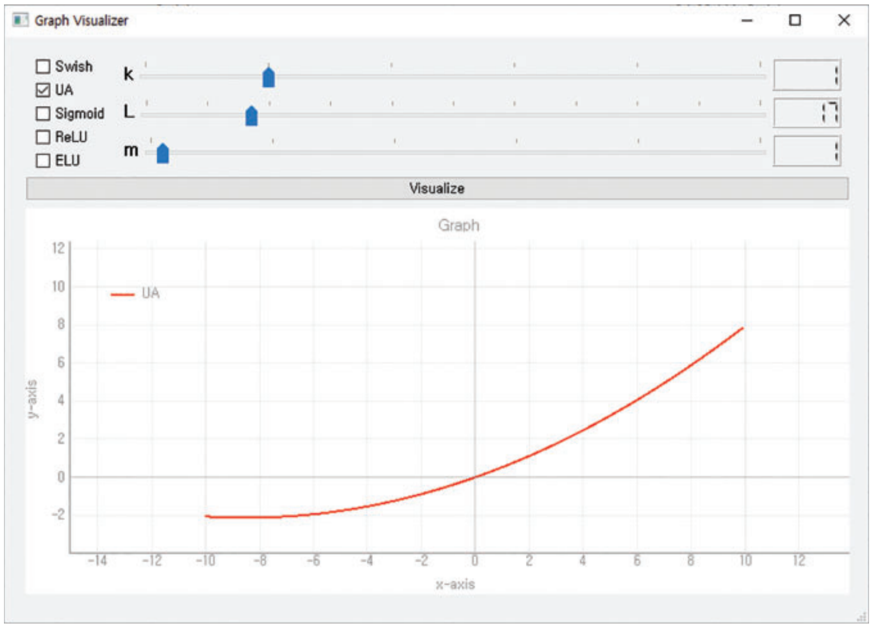

Figure 13: Graph of UA (k = 1, m = 1, L = 17)

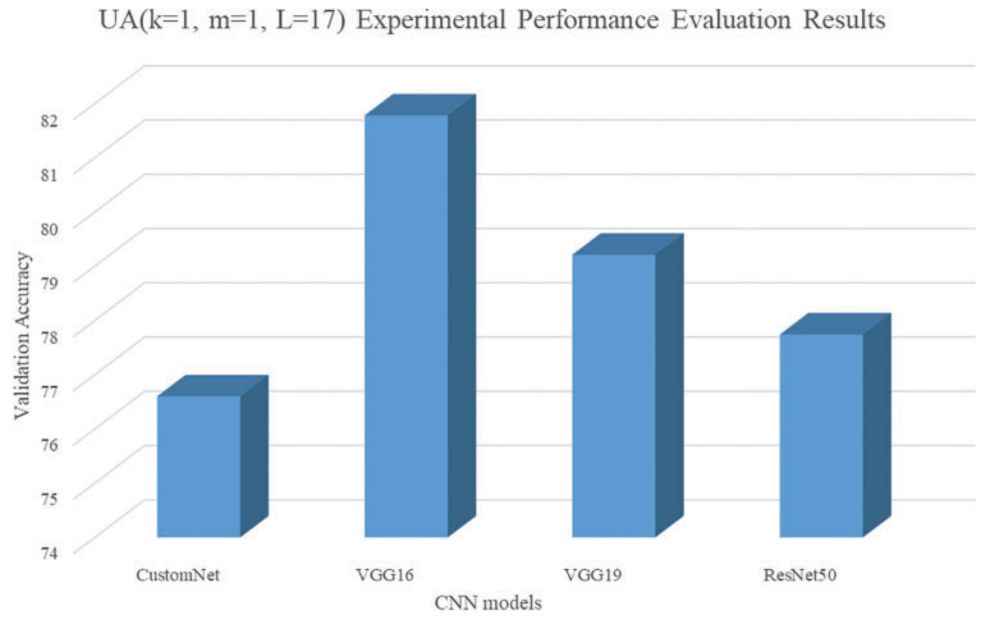

Figure 14: Results of UA ($k = 1$, $m = 1$, $L = 17$)

As a result of the third UA, CustomNet achieved 76.6% accuracy, unlike the application of the first and second UA, and improved accuracy by about 3.2% over the average accuracy of the models trained with the four activation functions. In the case of VGG16 and VGG19, there was a performance degradation of about 2.8% and 4.9%. For ResNet50, we achieved 77.74% accuracy and there was a loss of image features of the hidden layer, but there was a performance improvement of about 33.6%.

6 Conclusion

In this paper, the UA is proposed to improve the performance of deep learning and the usability of the activation function of researchers. The UA consists of three hyperparameters k, m, and L that determine the form of the activation function. By properly setting the hyperparameters, researchers can generate activation functions like traditional activation functions as well as various types of activation functions. We trained self-defined CNNs to minimize loss due to depth of neural networks by leveraging various benchmark datasets for comparison and experimental performance evaluation of traditional activation functions and UAs. As a result, the traditional activation function and the UA showed generally similar performance. In addition, three new types of activation functions were generated by changing the hyperparameters of the UA, and experimental performance evaluation was conducted using CIFAR10 and CNNs. In the experimental performance evaluation process, there were neural networks with improved performance for all three UAs, but there were also cases with improved performance in a specific neural network. Therefore, based on the results of this study, various researchers can easily generate and utilize new activation functions, so that technological advancement can be expected in various fields using deep learning. However, the traditional activation function was superior due to the complexity of the UA in terms of deep learning speed. In future studies, we will solve the problem of lowering the learning speed due to the complexity of the UA.

Acknowledgement: This work was supported by the National Research Foundation of Korea (NRF) grant funded by the Korea government (MSIT) (No. 2022R1F1A1062953).

Funding Statement: This work was supported by the National Research Foundation of Korea (NRF) grant funded by the Korea government (MSIT) (No. 2022R1F1A1062953).

Conflicts of Interest: The authors declare that they have no conflicts of interest to report regarding the present study.

References

[1] A. Krizhevsky, I. Sutskever and G. E. Hinton, "Imagenet classification with deep convolutional neural networks," *Advances in Neural Information Processing Systems*, vol. 25, pp. 1097–1105, 2012.

[2] K. Simonyan and A. Zisserman, "Very deep convolutional networks for large-scale image recognition," 2014. [Online]. Available: https://arxiv.org/abs/1409.1556

[3] C. Szegedy, W. Liu, Y. Jia, P. Sermanet, S. Reed *et al.,* "Going deeper with convolutions," in *Proc. Conf. on Computer Vision and Pattern Recognition*, Boston, MA, USA, pp. 1–9, 2015.

[4] K. He, X. Zhang, S. Ren and J. Sun, "Deep residual learning for image recognition," in *Proc. Conf. on Computer Vision and Pattern Recognition*, Las Vegas, NV, USA, pp. 770–778, 2016.

[5] T. Abbas, S. F. Ali, M. A. Mohammed, A. Z. Khan, M. J. Awan *et al.,* "Deep learning approach based on residual neural network and SVM classifier for driver's distraction detection," *Applied Sciences*, vol. 12, no. 13, pp. 6626, 2022.

[6] R. Girshick, J. Donahue, T. Darrell and J. Malik, "Rich feature hierarchies for accurate object detection and semantic segmentation," 2014. [Online]. Available: https://arxiv.org/abs/1311.2524

[7] J. Redmon, S. Divvala, R. Girshick and A. Farhadi, "You only look once: Unified, real-time object detection," in *Proc. Conf. on Computer Vision and Pattern Recognition*, Las Vegas, NV, USA, pp. 779–788, 2016.

[8] R. Girshick, "Fast R-CNN," in *Proc. of the IEEE Int. Conf. on Computer Vision*, NW Washington, DC United States, pp. 1440–1448, 2015.

[9] A. Bochkovskiy, C. Y. Wang and H. Y. M. Liao, "YOLOv4: Optimal speed and accuracy of object detection," 2020. [Online]. Available: https://arxiv.org/abs/2004.10934

[10] H. J. Mohammed, S. Al-Fahdawi, A. S. Al-Waisy, D. A. Zebari, D. A. Ibrahim *et al.,* "ReID-DeePNet: A hybrid deep learning system for person re-identification," *Mathematics*, vol. 10, no. 19, pp. 3530, 2022.

[11] O. I. Obaid, M. A. Mohammed, A. O. Salman, S. A. Mostafa and A. A. Elngar, "Comparing the performance of pre-trained deep learning models in object detection and recognition," *Journal of Information Technology Management*, vol. 14, no. 4, pp. 40–56, 2022.

[12] A. Bewley, Z. Ge, L. Ott, F. Ramos and B. Upcroft, "Simple online and realtime tracking," in *2016 IEEE International Conf. on Image Processing (ICIP)*, Phoenix, Arizona, USA, pp. 3464–3468, 2016.

[13] N. Wojke, A. Bewley and D. Paulus, "Simple online and realtime tracking with a deep association metric," in *2017 IEEE International Conf. on Image Processing (ICIP)*, Beijing, China, pp. 3645–3649, 2017.

[14] A. V. D. Oord, S. Dieleman, H. Zen, K. Simonyan, O. Vinyals *et al.,* "WaveNet: A generative model for raw audio," 2016. [Online]. Available: https://arxiv.org/abs/1609.03499

[15] Y. Ren, C. Hu, X. Tan, T. Qin, S. Zhao *et al.,* "FastSpeech 2: Fast and high-quality end-to-end text to speech," 2020. [Online]. Available: https://arxiv.org/abs/2006.04558

[16] J. Shen, R. Pang, R. J. Weiss, M. Schuster, N. Jaitly *et al.,* "Natural TTS synthesis by conditioning WaveNet on Mel spectrogram predictions," in *2018 IEEE International Conference on Acoustics, Speech and Signal Processing (ICASSP)*, Calgary, AB, Canada, pp. 4779–4783, 2018.

[17] J. Devlin, M. W. Chang, K. Lee and K. Toutanova, "BERT: Pre-training of deep bidirectional transformers for language understanding," in *Proc. 2019 Conf. of the North American Chapter of the Association for Computational Linguistics: Human Language Technologies*, Minneapolis, Minnesota, USA, vol. 1, pp. 4171–4186, 2019.

[18] A. Adhikari, A. Ram, R. Tang and J. Lin, "DocBERT: BERT for document classification," 2019. [Online]. Available: http://arxiv.org/abs/1904.08398

[19] I. Beltagy, K. Lo and A. Cohan, "SciBERT: A pretrained language model for scientific text," in *Proc. 2019 Conf. on Empirical Methods in Natural Language Processing and the 9th Int. Joint Conf. on Natural Language Processing (EMNLP-IJCNLP)*, Hong Kong, China, pp. 3615–3620, 2019.

[20] A. K. Das, D. Mishra, K. Das, A. K. Mohanty, M. A. Mohammed *et al.,* "A deep network-based trade and trend analysis system to observe entry and exit points in the forex market," *Mathematics*, vol. 10, no. 19, pp. 3632, 2022.

[21] A. Iliev, N. Kyurkchiev and S. Markov, "On the approximation of the step function by some sigmoid functions," *Mathematics and Computers in Simulation*, vol. 133, pp. 223–234, 2017.

[22] A. Hamidoglu, "On general form of the tanh method and its application to nonlinear partial differential equations," *Numerical Algebra Control and Optimization*, vol. 6, no. 2, pp. 175–181, 2016.

[23] V. Nair and G. E. Hinton, "Rectified linear units improve restricted boltzmann machines," in *Proc. 27th Int. Conf. on Machine Learning (ICML)*, Haifa, Israel, pp. 1–8, 2010.

[24] K. He, X. Zhang, S. Ren and J. Sun, "Delving deep into rectifiers: Surpassing human-level performance on imagenet classification," in *Proc. IEEE Int. Conf. on Computer Vision*, Santiago, Chile, pp. 1026–1034, 2015.

[25] B. Xu, N. Wang, T. Chen and M. Li, "Empirical evaluation of rectified activations in convolutional network," 2015. [Online]. Available: https://arxiv.org/abs/1505.00853

[26] M. Anthimopoulos, S. Christodoulidis, L. Ebner, A. Christe and S. Mougiakakou, "Lung pattern classification for interstitial lung diseases using a deep convolutional neural network," *IEEE Transactions on Medical Imaging*, vol. 35, no. 5, pp. 1207–1216, 2016.

[27] S. Scardapane, S. Van Vaerenbergh, A. Hussain and A. Uncini, "Complex-valued neural networks with nonparametric activation functions," *IEEE Transactions on Emerging Topics in Computational Intelligence*, vol. 4, no. 2, pp. 140–150, 2018.

[28] D. A. Clevert, T. Unterthiner and S. Hochreiter, "Fast and accurate deep network learning by exponential linear units (ELUs)," 2015. [Online]. Available: https://arxiv.org/abs/1511.07289

[29] Y. Yu, K. Adu, N. Tashi, P. Anokye, X. Wang *et al.,* "RMAF: Relu-memristor-like activation function for deep learning," *IEEE Access*, vol. 8, pp. 72727–72741, 2020.

[30] Z. Qiumei, T. Dan and W. Fenghua, "Improved convolutional neural network based on fast exponentially linear unit activation function," *IEEE Access*, vol. 7, pp. 151359–151367, 2019.

[31] H. Zhao, F. Liu, L. Li and C. Luo, "A novel softplus linear unit for deep convolutional neural networks," *Applied Intelligence*, vol. 48, no. 7, pp. 1707–1720, 2018.

[32] F. Godin, J. Degrave, J. Dambre and W. De Neve, "Dual rectified linear units (DReLUs): A replacement for tanh activation functions in quasi-recurrent neural networks," *Pattern Recognition Letters*, vol. 116, pp. 8–14, 2018.

[33] A. Krizhevsky and G. Hinton, "Learning multiple layers of features from tiny images," 2009. [Online]. Available: http://citeseerx.ist.psu.edu/viewdoc/download?doi=10.1.1.222.9220&rep=rep1&type=pdf

[34] D. P. Kingma and J. Ba, "Adam: A method for stochastic optimization," 2014. [Online]. Available: https://arxiv.org/abs/1412.6980